RESEARCH ARTICLE

Check for updates

Unraveling the phenotypic and metabolic responses induced by urea-encapsulated hydrogel beads on *Brassica juncea* (L.) Czern & Coss†

Muthumari Balakrishnan,[ab] Vignesh Kumar Balasubramanian,[b] Kavitha Murugan,[a] John Praveen Kumar John Kennedy,[a] Subashri Dhanasekaran,[b] Shih-Feng Fu,[b] Shang-Tse Ho,[c] Jothi Basu Muthuramalingam [iD] ‡*[d] and Jui-Yu Chou‡*[b]

Hydrogels, three-dimensional polymeric networks capable of absorbing and retaining significant amounts of aqueous solution, offer a promising platform for controlled release of desired compounds. In this study, we explored the effects of urea delivery through galactoxyloglucan–sodium alginate hydrogels on the phenotypic and metabolic responses of *Brassica juncea*, a vital oilseed and vegetable crop. The experiments were conducted with four treatments: control (without hydrogel beads and urea), direct urea supplementation (U), hydrogel beads with urea (HBWU), and hydrogel beads without urea (HBWOU). Our findings revealed that HBWU-treated plants exhibited commendable plant growth with significantly higher chlorophyll content (11.06 mg/0.1 g) compared to the control (3.67 mg/0.1 g) and U-treated group (6.41 mg/0.1 g). Metabolic analysis identified 17 major intra-cellular metabolites involved in nitrogen metabolism. HBWU treatment significantly boosted nitrogen assimilation in plants, as evidenced by the upregulation of 9 metabolites. Furthermore, a proposed schematic diagram illustrates the HBWU induced-metabolic pathways and nitrogen metabolism in *B. juncea*. These findings demonstrate the potential of hydrogel-based controlled-release systems to enhance plant growth and nitrogen assimilation.

1. Introduction

Biopolymers, naturally occurring macromolecules derived from non-fossil biological sources, have garnered substantial attention as promising alternatives to synthetic polymers due to their inherent advantages, including biocompatibility, abundance, and biodegradability.[1] Among these biological sources, plant-based biopolymers, especially polysaccharides, are emerging as promising renewable resources due to their abundance and continuous replenishment.[2] Galactoxyloglucan (GXG) is a neutral hemicellulose abundantly found in the seed storage wall of *Tamarindus indica* L., a member of the Fabaceae family. The biopolymer, GXG consists of a β-D-(1 → 4) glucan backbone with α-D-(1 → 6) xylopyranosyl residues attached as side chains.

These xylopyranose side chains are further substituted with β-D-(1 → 2) galactopyrosyl residues.[3] Similarly, algin or alginic acid is a naturally occurring, insoluble structural polysaccharide prevalent in the cell wall and intercellular matrix of brown algae, such as *Sargassum* sp. Sodium alginate (SA) is a derivative of alginic acid and which is often referred as a block copolymer composed of two anionic monomers: 1,4-linked β-D-mannuronate (M) and α-L-guluronate (G) residues. Both GXG and SA biopolymers demonstrate promising applications in the food, pharmaceutical, biomedical, industrial, and agricultural sectors.[4,5] As SA is renowned for its hydrogel-forming capabilities, it exhibits distinctive gelation properties, forming hydrogels upon interaction with divalent metal cations.[6]

Hydrogels are three-dimensional networks of hydrophilic polymers cross-linked by covalent bonds or other physical interactions, characterized by their high flexibility, swelling and water retention capacity.[7] Owing to their unique attributes, hydrogels have attracted considerable attention from researchers as a versatile platform for applications across various fields. In agriculture and horticulture, hydrogels are particularly valued for their controlled and sustained delivery of agrochemicals and their potential as biofertilizers through the encapsulation of plant growth-promoting microorganisms, ultimately leading to increased crop yields.[8] While inorganic fertilizers like nitrogen,

a Department of Botany, Alagappa University, Karaikudi, 630 003, India

b Department of Biology, National Changhua University of Education, Changhua 500, Taiwan. E-mail: jackyjau@cc.ncue.edu.tw

c Department of Wood Based Materials and Design, College of Agriculture, National Chiayi University, Chiayi 600, Taiwan

d Centre for Distance and Online Education, Alagappa University, Karaikudi, 630 003, India. E-mail: jothibasum@alagappauniversity.ac.in

† Electronic supplementary information (ESI) available. See DOI: https://doi.org/10.1039/d4mo00192c

‡ Equal contribution.

phosphorus, and potassium have been pivotal in boosting crop yields, the growing scarcity of nitrogen resources presents a major hurdle for sustainable agriculture.[9] Urea (U), a widely used inorganic nitrogen fertilizer with a high nitrogen content and relatively low production cost, has been a cornerstone of agricultural practices.[10] However, the overuse and prolonged application of urea fertilizer have led to significant environmental problems, including volatilization, runoff, nitrate leaching, and soil infertility. Hence, hydrogels are emerging as a promising solution for nitrogen management, and tend to release urea in a slow or controlled manner.[9]

Nitrogen is a critical macronutrient for plant growth and development, essential for the synthesis of amino acids, proteins, nucleic acids, lipids, chlorophyll, and other vital biomolecules.[11] Vascular plants primarily absorb nitrogen in the form of nitrate, ammonium (inorganic), and organic nitrogen (urea) from soil.[12] Moreover, urea plays a pivotal role in nitrogen metabolism, serving as an intermediate in both arginine degradation and ureide catabolism. Within mitochondria, arginine is broken down by arginase, contributing to nitrogen recycling following protein degradation. The resulting urea can be further metabolized in the cytoplasm by urease, yielding ammonium (NH_4^+), which is subsequently assimilated into glutamine. Alternatively, urea can originate from the catabolism of purines or ureides such as allantoate and allantoin, which are primarily found in legumes for long-distance N transport.[13] To adapt to varying nitrogen availability and environmental conditions, plants have evolved sophisticated mechanisms to regulate their nitrogen metabolism. Metabolites, the end products of cellular processes, serve as valuable phenotypic markers, offering insights into the intricate pathways underlying agronomically relevant traits and their responses to stress.[14] By identifying and quantifying metabolites, researchers can gain insights into plant biology. This approach is particularly valuable for studying the effects of nitrogen nutrition on plant growth, development, and stress tolerance.[15]

This study was undertaken to investigate the impact of controlled urea release on *Brassica juncea*, an economically important crop that serves as both an oilseed and a vegetable. The research focused on utilizing urea-encapsulated GXG–SA hydrogels as a novel method for delivering nitrogen to the plants. The primary objective was to assess how this controlled release mechanism influences various aspects of plant growth, development, and the underlying metabolic processes. By providing a steady and sustained supply of urea, the hydrogels are hypothesized to improve nitrogen use efficiency, potentially leading to enhanced plant health and productivity. To gain a comprehensive understanding of the metabolic changes associated with this controlled urea release, the study involved a comparative analysis. We examined the effects of urea delivered *via* GXG–SA hydrogels in contrast to the conventional method of direct urea application. This comparison is crucial in determining whether the hydrogel-mediated approach offers distinct advantages in optimizing nitrogen utilization, promoting better growth outcomes, and influencing the metabolic pathways in *B. juncea*. Ultimately, the findings from this research could provide valuable insights into the development of more sustainable and effective fertilization strategies for important crops.

2. Materials and methods

2.1. Materials

Urea (carbamide) was purchased from SRL (Sisco Research Laboratories Pvt. Ltd Mumbai, India). Calcium chloride ($CaCl_2$) anhydrous was purchased from HiMedia Laboratories Pvt. Ltd Mumbai, India. Acetone extra-pure was purchased from Santoku Chemical Company, Ltd Japan. Methanol extra-pure was purchased from M & J Scintek Co., Ltd Taiwan. Methoxyamine pyridine hydrochloride and *N,O*-bis(trimethylsilyl)trifluoroacetamide (BSTFA) was purchased from Morchem Shanghai Trading Co., Ltd China. *Sargassum* sp., was collected from the Pamban Coastal Area (Latitude – 9°16.6630'N, Longitude – 79°12.2980'E), Ramanathapuram, Tamil Nadu, India. *Tamarindus indica* L. seeds were purchased from the local market in Karaikudi, Tamil Nadu, India.

2.2. Biopolymers extraction, characterization and hydrogel bead optimization

The extraction of GXG from the seeds of *T. indica* and SA from *Sargassum* sp. were done accordingly as described in previous articles.[16,17] Briefly, GXG was extracted through a multi-step process involving seed decortication, pulverization, defatting, deproteination, and ethanol precipitation. Decortication and pulverization were achieved using microwave heating (1000 W for 120 seconds), followed by water soaking (1:4 w/v) for 8 hours, drying at 100 °C for 4 hours, and subsequent pulverization. Conventional methods were employed for defatting, deproteination, and ethanol precipitation. The resulting precipitate was air-dried at 60 °C for 8 hours, then ground into a fine powder, and stored at −20 °C.[16,17] Extraction of SA was conducted using a four-step process involving calcium chloride treatment, acid treatment, alkaline treatment, and precipitation. Following precipitation, the samples were dried at 50 °C for 3 hours, ground into a fine powder, and stored at −20 °C.[18] Further, GXG and SA were characterized and confirmed by Ultraviolet (UV)-visible spectroscopy (Labman scientific instruments PVT. Limited, Model no: LMSP-UV1000B), Fourier transform infrared spectroscopy (FT-IR) analysis (Bruker, Alpha II-Model Advanced, Berlin, Germany), and Nuclear magnetic resonance (NMR) analysis using Bruker Avance NEO NMR spectrophotometer at 298 K. Furthermore, GXG–SA blended hydrogel beads were prepared using the ionotropic gelation method. The optimal biopolymer concentration, crosslinker concentration, and crosslinking time were optimized based on the swelling attributes of the hydrogel. The optimized biopolymer formulation was GXG (2%)–SA (1.5%), crosslinker concentration (0.1 M $CaCl_2$) and crosslinking time (15 min) which were elaborately described in previous study.[19] For optimizing urea encapsulation, hydrogel beads were prepared with varying urea concentrations (0.1%, 0.5%, 1%, 1.5%, 2%, and 2.5%). The optimal concentration was selected based on the highest urea release rate and favourable swelling properties. The optimized formulation, GXG (2%)–U (2%)–SA (1.5%), was utilized in this research. The optimization of urea-encapsulated hydrogel beads and their release kinetics were thoroughly investigated in recent publication.[20]

2.3. Preparation of urea encapsulated GXG–SA hydrogel beads

For the hydrogel preparation, SA (1.5% w/v) was dissolved in distilled water and homogenized using a magnetic stirrer at 600 rpm and 30 °C for 30 minutes to achieve through mixing. Meanwhile, U (2% w/v) was then added,[9,21,22] followed by the gradual addition of GXG (2% w/v) to the SA–U mixture. The mixture was further homogenized using a magnetic stirrer at 1000 rpm and 30 °C for 3 hours. Subsequently, the mixture was added dropwise to a 0.1 M $CaCl_2$ crosslinking solution using a syringe over 15 minutes (Fig. 1). The resulting beads were filtered, washed three times with distilled water, and air-dried at room temperature for 48 hours.[19]

2.4. Characterization and urea content determination of urea encapsulated GXG–SA hydrogel beads

The prepared hydrogel beads GXG (2%)–U–SA (1.5%) were characterized through FT-IR. The measurements were observed after scanning over (24 scans per sample) with the absorbance spectral wavelength ranging between 400–5000 cm^{-1}.

The urea content in the prepared hydrogel beads was analyzed using the diacetyl-monoxime method, as described in the referenced article,[23] with measurements taken on using Ultraviolet-visible spectrophotometer.

2.5. Evaluation of urea encapsulated GXG–SA hydrogel beads on *Brassica juncea*

2.5.1. Plant samples and growth conditions. Commercially purchased *B. juncea* (L.) Czern & Coss. (Mustard plants) were grown individually in pots filled with horticultural compost (Universal potting soil, FERTIPLUS, Helmond, The Netherlands) as a planting medium. This compost having high organic matter content, consisting of both white and black peat, plays a significant role in influencing the soil and its suitability for plant growth. This substrate was selected for its ability to support seedling establishment and promote uniform growth. However, peat, being naturally low in nitrogen compared to other organic materials like compost or manure, may not provide sufficient nitrogen to meet the plants nutritional needs.[24,25] Two-week-old plants were maintained in a controlled environment chamber at 22 °C with a light intensity of 2400–2500 Lux, following a 16-hour light/8-hour dark cycle. The plants were irrigated with tap water at regular intervals across all treatments.

2.5.2. Treatments. The experiment was designed with four treatments; control (C) without urea and hydrogel, direct urea supplementation (U), hydrogel bead with urea (HBWU) and hydrogel bead without urea (HBWOU). For the hydrogel treatments, 50 mg of hydrogel beads were applied, and for the urea group, 16 mg of urea was used (based on predetermined urea concentration). There were 32 experimental units, with 8 plants in each group. After 35 days of treatment, the plants were harvested for further analysis (Fig. 1).

2.5.3. Phenotypic and bio-active compound analysis. For phenotypic analysis, the entire plant was carefully harvested and washed with running tap water. Subsequently, their fresh
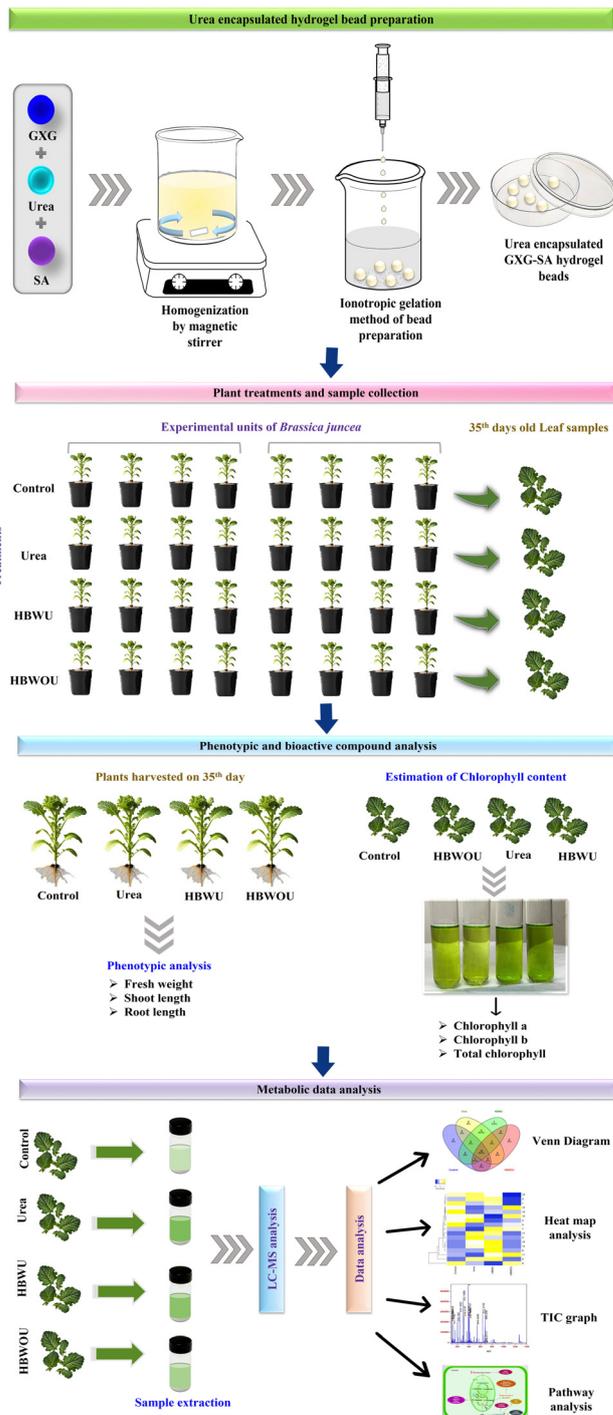

Fig. 1 A schematic summary of overall methodology employed in this study.

weight, root length, and shoot length were measured.[26] For the analysis of bioactive compounds, fresh leaves were harvested and used for chlorophyll estimation by following the acetone method (Fig. 1). Specifically, 0.1 g of leaves were accurately weighed and ground with 2 mL of 80% ice-cold acetone. The volume was then adjusted to 10 mL using 80% acetone. The chlorophyll content was assessed through spectrophotometric

analysis, with optical density (OD) values measured at wavelengths of 663 nm and 645 nm. A solution of 80% acetone was used as the blank for this analysis. The amount of chlorophyll (mg g^{-1}) present in the plant extract was calculated by using the formula as described in the reference article.[27]

2.6. Metabolomic profiling of *Brassica juncea* treated with urea encapsulated GXG–SA hydrogel beads

2.6.1. Sampling and quenching of the intra-cellular metabolites. Leaf samples (1 g) of *B. juncea* were collected from the control, urea, HBWU, and HBWOU test groups. The samples were ground using a pre-chilled mortar and pestle with liquid nitrogen. The resulting powder was transferred to a 50 mL centrifuge tube containing 20 mL of 60% pre-chilled methanol at −80 °C.[28] Quenching of the metabolism was done in 15–30 seconds. Then, the mixture was centrifuged at 8500 rpm for 5 minutes at −4 °C. The samples were stored at −80 °C until further analysis.[29–31]

2.6.2. Extraction of the intra-cellular metabolites. The samples were retrieved from the −80 °C after 48 hours, suspended with 2.5 mL of ice-cold methanol–water solution (1 : 1), thawed in an ice bathtub for 5 minutes, then rigorously vortexed for a couple of minutes, and frozen in −80 °C for 30 minutes. This cycle was repeated thrice and centrifuged at 10 000 rpm for 20 minutes at −20 °C. An additional 2.5 mL of ice-cold methanol–water solution was added to the cell pellets and combined with the former. This supernatant was lyophilized at −80 °C condensation with a 1.000 Pa vacuum for 24 hours and used for further liquid chromatography-mass spectrometry (LC-MS) analysis.[28,31–33]

2.6.3. Derivatization of intra-cellular metabolites. The samples were subjected to a two-step derivatization procedure. Firstly, 200 μL of methoxyamine pyridine hydrochloride was mixed with the sample for 30 seconds and incubated at 37 °C for 90 minutes without disturbances. Secondly, 200 μL of *N,O*-bis(trimethylsilyl)trifluoroacetamide (BSTFA) were added to the mixture, incubated at 70 °C for 30 minutes, and incubated at room temperature for 30 minutes. The derivatized samples were transferred to an LC-MS vial for analysis.[30,31,34]

2.6.4. LC-MS analysis. The LC-MS analysis was performed using an Agilent LC/Q-TOF 6546 system, equipped with a dual AJS-E.S.I. source for ionization. The mobile phases consisted of ultrapure water and LC-MS grade acetonitrile, both containing 0.1% formic acid. Separation was achieved using an acquity UPLC® BEH C18 column (2.1 mm × 100 mm, 1.7 μm particle size), with the column oven set to 40 °C. Key mass spectrometer parameters were as follows: sheath gas temperature at 350 °C with a flow rate of 11.0 L min^{-1}, fragmentor voltage at 140 V, capillary voltage at 3.5 kV, and nebulizer pressure at 40 psi. The gas temperature was set to 320 °C with a flow rate of 12 L min^{-1}, while the collision energy was set at 20 eV. The ion spray voltage was set to 0 V. The MS1 scan range was *m/z* 100–1700, and the MS2 scan range was *m/z* 20–1700, with a scan speed of 5 spectra per s and an absolute threshold of 500 counts. Mass tolerance was set at 20 ppm. Functional metabolites abundance differences were assessed using the KEGG Database and the heat map generated using HemI 2.0.[29,31,35–37]

2.7. Statistical analysis

All the data are presented as mean ± standard error and analysed using Microsoft Excel 2010. The graphs were plotted using Origin Pro 8.5, and the analysis of variance (ANOVA) were analysed using IBM SPSS statistics Version 25. Hierarchical cluster analysis was performed using the bioinformatics online platform Heatmapper. Correlation of up-regulated and down-regulated metabolites was assessed using the bioinformatics tool Venn Diagram Webtools.

3. Results

3.1. Characterization and urea content determination of urea encapsulated GXG–SA hydrogel beads

The functional groups of the biopolymers and urea within the hydrogel beads was analyzed using FT-IR (Fig. S1, ESI†). The characteristic peaks of urea, GXG, and SA were identified and compared to standard spectra as in the literature.[17,19] The presence of urea was confirmed by the observation of C–N and C=O stretching peaks at 1444.38 cm^{-1} and 1583.10 cm^{-1}, respectively, along with NH$_2$ stretching at 3469.32 cm^{-1}.[10,38] The anomeric group of SA and GXG (β-(1 → 4) glycosidic linkages) was indicated by a peak at 758.01 cm^{-1}, while uronic acid residues of SA were evident at 947.91 cm^{-1} and 1036.86 cm^{-1}. Additionally, the C–O bending and C–H stretching peaks of GXG appeared at 1294.50 cm^{-1} and 1482 cm^{-1}, respectively. These findings collectively support the successful incorporation of biopolymers into the hydrogel beads.[19,21,39]

Spectrophotometric analysis was performed to quantify the urea concentration in the hydrogel beads. A calibration curve was generated using known concentrations of commercial urea (0.1 to 1 g). The results showed that approximately 0.030 ± 0.001 g of urea was entrapped per 0.1 g of hydrogel beads.

3.2. Evaluation of urea encapsulated GXG–SA hydrogel beads on *Brassica juncea*

3.2.1. Effect of urea encapsulated GXG–SA hydrogel beads on plant growth. *B. juncea* commonly known as mustard, was selected as the model plant for this study due to its agronomic and economic importance as a vital oilseed and vegetable crop cultivated widely across the globe, particularly in regions with significant agricultural activity.[40] The effect of urea encapsulated hydrogel beads on phenotypic variations in leaves were observed across all four treatments (Fig. 2) with quantitative growth parameters summarized in (Table 1). Compared to the control group, which received neither hydrogel beads nor urea, plants treated with HBWU (2% GXG, 2% urea, 1.5% SA) exhibited significant increases in fresh weight, shoot length with, root length and the leaves are seen as dark green colour. These findings demonstrate the beneficial effects of these hydrogel beads on *B. juncea* plant growth and development. Meanwhile, HBWOU (2% GXG, 1.5% SA) treated plants showed pale yellow green leaves with improved growth parameters compared to the control and urea-only groups, plants exhibited the lowest fresh weight and shoot length. However, root length was notably

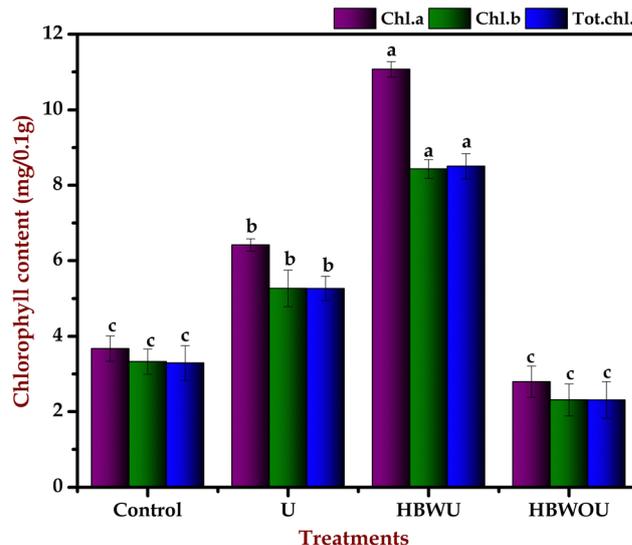Fig. 2 Phenotypic variations in leaf colour of *B. juncea* treated with urea-encapsulated hydrogel beads.

Fig. 3 Effect of urea-encapsulated hydrogel beads on chlorophyll content in *B. juncea* leaves. Different letters above the bars indicate statistically significant difference at $P < 0.05$.

increased in urea-treated plants (Table 1), indicating a specific influence on root development.

Previous studies have shown a positive correlation between nitrogen fertilization and the development of biomass, roots, and shoots.[9,41] However, excessive direct application of urea can negatively impact plant growth.[42] The results of this study indicated that hydrogel beads significantly enhanced fresh weight, shoot length, and root length in *B. juncea* plants compared to the control group and urea alone treated group. The controlled-release mechanism of urea from the hydrogel beads may have contributed to these positive effects on plant growth, as opposed to the direct application of urea, which has been shown to reduce growth rates.[43]

3.2.2.   Effect of urea encapsulated GXG–SA hydrogel beads on bioactive compounds. Chlorophylls are a group of naturally occurring pigments that give plants their green color. While they are essential for photosynthesis and also it is recognized as prominent bioactive compound.[44] The depicted (Fig. 3) illustrates shows the effect of HBWU hydrogel beads treatment on the chlorophyll content in *B. juncea* leaves, compared with control, urea supplemented, HBWOU group. Plants treated with HBWU exhibited significantly higher levels of chlorophyll *a* (11.06 mg/0.1 g) and chlorophyll *b* (8.43 mg/0.1 g) compared to the control group (3.67 mg/0.1 g and 3.32 mg/0.1 g, respectively) and all other treatments. While urea-treated plants showed the second-highest total chlorophyll content (5.26 mg/0.1 g), these results suggest that the urea encapsulated hydrogel beads may be more effective in increasing chlorophyll concentration than urea alone.[45,46] Notably, plants treated with HBWOU exhibited the minimal chlorophyll content (2.30 mg/0.1 g), possibly due to the absence of urea.

Previous studies have demonstrated that nitrogen supplementation can enhance photosynthesis by increasing photosynthetic enzyme activity, chlorophyll content, and composition.[15] While the urea-only supplemented groups showed elevated chlorophyll concentrations, it was notably observed that HBWU treated plants exhibited efficient chlorophyll content, potentially due to the controlled release of urea. Although GXG–SA hydrogel treatment alone had minimal effects on chlorophyll composition however, it was found to significantly improve plant biomass, root, and shoot development.[47,48]

3.3.   Metabolomic profiling of *Brassica juncea* treated with urea-encapsulated GXG–SA hydrogel beads

Upon the conclusion from the phenotypic responses, the study hypothesized that urea encapsulated in GXG–SA hydrogel beads would enhance plant growth and metabolism in *B. juncea* by providing a controlled and sustained release of nitrogen compared to conventional urea application methods. This encapsulation was expected to improve nitrogen assimilation and modulate key metabolites involved in nitrogen metabolism, thereby offering a sustainable approach to agriculture. Hence, the metabolic profiling was conducted using LC-MS analysis.

The LC-MS analysis (Fig. S2–S5, ESI†) revealed the significant involvement of intracellular metabolites in urea metabolism within plants, which plays a critical role in enhancing plant growth.

Table 1 Phenotypic parameters of *B. juncea* after 35 days of treatments. Different letters (superscript) indicate the statistically significant difference at $P < 0.05$

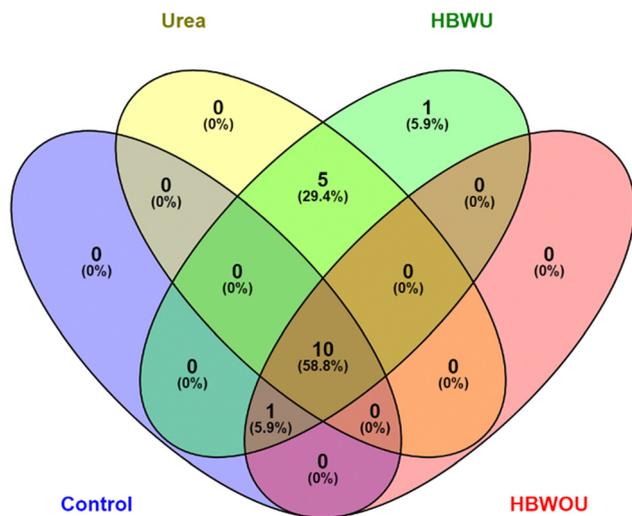| Treatments	Control	U	HBWU	HBWOU
Fresh weight (g)	3.16 ± 0.11^{b}	2.8 ± 0.10^{c}	3.45 ± 0.44^{a}	3.27 ± 0.07^{ab}
Root length (cm)	17.12 ± 1.41^{bc}	16.92 ± 1.22^{c}	30.12 ± 5.26^{a}	26.55 ± 3.33^{bc}
Shoot length (cm)	3.22 ± 0.22^{bc}	4.17 ± 0.04^{ab}	4.18 ± 0.03^{a}	3.02 ± 0.09^{c}

Fig. 4 Venn diagrammatic representation of up and down-regulated metabolites across all the treated groups of plants.

Fig. 5 Hierarchical cluster analysis of up and down-regulated metabolites in all the treated groups of plants.

The study identified seventeen major intracellular metabolites associated with the urea metabolic pathway (Table S1, ESI†). Among these, nine metabolites were upregulated in plants treated with HBWU compared to the control group, mirroring the pattern observed in plants directly treated with urea. Furthermore, ten metabolites were upregulated in HBWU-treated plants compared to those treated with direct urea, and eleven metabolites showed increased levels when compared to plants treated only with HBWOU, relative to control groups. Notably, seven metabolites were downregulated in HBWU-treated plants compared to the control group (Fig. 4) shows the detection of all seventeen metabolites across the treated and control groups. A total of 58.4% of the metabolites were detected in all groups. Additionally, 29.4% of the metabolites were found only in the two groups treated with urea (HBWU and urea-treated plants). One metabolite (5.9%) was detected in all groups except the urea-treated ones, while another 5.9% was detected exclusively in the HBWU-treated plants.

Urea, a well-known plant growth-promoting substance, can be absorbed through the roots from the soil or synthesized internally *via* arginine catabolism through the action of arginase.[49] As a primary nitrogen source, urea is integrated into plant metabolism and essential for growth and development. Upon entering the plant cell, urea undergoes hydrolysis by the enzyme urease, yielding ammonia and carbon dioxide.[50] The resulting ammonia is assimilated into amino acids, which are crucial for protein synthesis, chlorophyll production, and nucleic acid formation.[51] Efficient urea metabolism is essential for optimizing plant growth, yield, and nitrogen use efficiency despite mitigating environmental impacts such as nitrogen leaching and greenhouse gas emissions. Several factors, including soil pH, microbial activity, plant species, and other ecological conditions, influence urea metabolism.

The study further demonstrated that urea supplementation through both hydrogel beads and direct application led to significant activation of the glutamine synthetase/glutamine:2-oxoglutarate amidotransf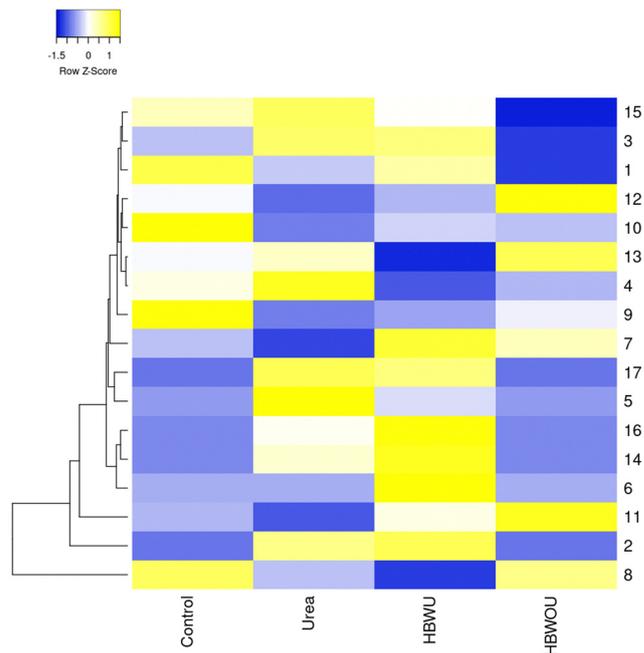erase (GS/GOGAT) cycle. The GS/GOGAT pathway begins with the assimilation of ammonia, derived from urea, into glutamine and then into glutamate.[51] This ammonium ion is primarily assimilated in chloroplasts *via* the GS/GOGAT pathway.[14] In higher plants, two major isoforms of GS are present: GS1, localized in the cytosol, and GS2, located in plastids. GS1 plays a critical role in leaf senescence and the synthesis of glutamine, which is transported through the phloem sap, while GS2 is involved in photorespiration.[14,52] Plastid-localized GS catalyzes the ATP-dependent conversion of glutamate and ammonia into glutamine. This glutamine then reacts with 2-oxoglutarate (2-OG), producing two molecules of glutamate.[14] Hierarchical cluster analysis revealed that the presence of high levels of glutamate was detected in plants treated with HBWU and direct urea, with negligible amounts found in the HBWOU and control treatments, probably due to the limited availability of urea in the soil or environment (Fig. 5 and Fig. S6, ESI†). Glutamate is the central molecular in amino acid metabolism in plants and acts as the substrate for the production of glutamine-by-glutamine synthetase.[52] Conversely, glutamine levels were higher in the control group, followed by HBWU, direct urea, and HBWOU treatments. The control group exhibited glutamine levels 1-fold higher than HBWU, 1.5-fold higher than direct urea, and 2.2-fold higher than HBWOU. This indicates that limited urea supplementation in the control and HBWOU treatments slowed the conversion of glutamine to glutamate. In contrast, abundant urea in the HBWU and urea-treated plants accelerated the glutamate conversion. Glutamine in the higher plants was produced from the conversion of glutamate by enzymes, and glutamate levels fell.[53]

Notably, glutamate levels in HBWU were 1.5-fold higher than in plants treated with direct urea. *N*-Carbamyl-ʟ-glutamate, an intermediate in urea metabolism and a precursor
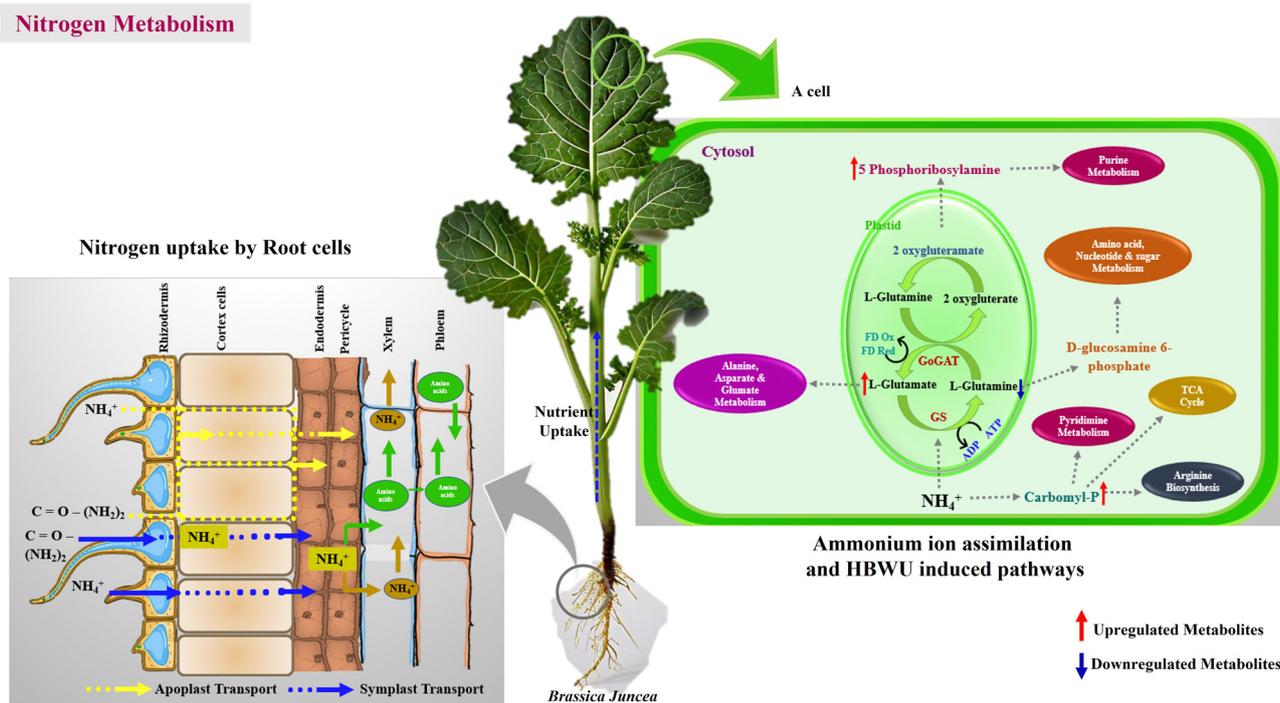
Fig. 6 A schematic representation of proposed HBWU-induced metabolic pathway and nitrogen metabolism in *B. juncea*.

for arginine biosynthesis, was also more abundant in urea-treated plants, followed by HBWU-treated plants. Specifically, *N*-carbamyl-L-glutamate levels were 2-fold higher in HBWU than in HBWOU and 1.5-fold higher than in the control group, with a similar trend observed in urea-treated plants. *N*-Carbamyl-L-glutamate is involved in the process of histidine production and is also directly involved in seed aging and low-vigor seed proliferation.[54] 2-Oxoglutarate, a key obligatory intermediate metabolite in urea metabolism, was also detected. This metabolite is involved in several crucial metabolic pathways, including the tricarboxylic acid cycle (TCA cycle), pentose and glucuronate interconversions, ascorbate and arginine biosynthesis, alanine, aspartate and glutamate metabolism, lysine biosynthesis and degradation, histidine metabolism, and various other pathways related to secondary metabolites, antibiotics, and plant hormones including gibberellin which directly plays a role in early senescence and ripening of the fruits.[55]

Carboxyphosphate, an intermediate product and also rate limiting factor of PEP carboxylase reaction, was present across all treatments at similar levels, with a slightly higher concentration in plants treated with HBWU and HBWOU compared to the control and urea treatments. This could be attributed to the polysaccharide compounds present in the hydrogel beads.[56] Similarly, ADP levels were elevated in plants treated with hydrogel beads, as ADP is a product of phosphorylation. Carboxyphosphate reacts with ammonia to produce carbamic acid, which then reacts with ATP to form carbamyl phosphate and ADP.[57] The levels of carbamyl phosphate were comparable across all treatments, with no significant differences observed.

D-Glucosamine 6-phosphate, involved in nucleotide sugar biosynthesis and alanine, aspartate, and glutamate metabolism, was

identified in all treatments but showed reduced levels in HBWU, followed by control, urea, and HBWOU.[58] 5-Phosphoribosylamine, a crucial metabolite in purine metabolism, was found in abundance −2-fold higher in HBWU and 1-fold higher in urea-treated plants, with minimal production in the control and HBWOU groups. This metabolite plays an essential role in purine metabolism, secondary metabolite biosynthesis, and alanine, aspartate, and glutamate metabolism.[59] Similarly, 2-oxoglutaramate, a transamination product of glutamine, another important metabolite with roles analogous to 5-phosphoribosylamine, was detected in HBWU and urea-treated plants.[60,61]

5′-Phosphoribosylglycinamide, an intermediate in purine metabolism derived from ribose, was found in high abundance-5-fold higher in HBWU and 2-fold higher in urea-treated plants, with no or very low levels detected in the control and HBWOU groups.[59] Deoxyinosine, a key metabolite in purine and nucleotide metabolism and a facilitator of adenosine nucleoside uptake *via* ABC transporters, was abundant in HBWU and urea-treated plants.[62]

In addition to these metabolites, intracellular nutrient metabolites such as NAD^+, $NADP^+$, NADPH, ATP, ADP, and NADH were detected, with higher concentrations observed in HBWU and urea-treated plants compared to control and HBWOU treatments. The abundance of these metabolites indicates a sustained cyclization of metabolic pathways, thereby enhancing plant growth and development, as evidenced by phenotypic characteristics.

Overall, this study revealed the impact of urea application on plant metabolism using LC-MS analysis. The data suggest that urea supplementation, particularly *via* HBWU, promotes the activation of the urea metabolic pathway, leading to increased

levels of key metabolites associated with nitrogen assimilation, purine biosynthesis, and energy metabolism. Based on these results, the possible schematic metabolic pathway has been elucidated for HBWU treated plants. Differences in the intracellular metabolites and the metabolic path are represented, indicating the red colour upside arrow for the upregulation of intracellular metabolites and the blue colour downside arrow for the downregulation of intracellular metabolites (Fig. 6). These findings contribute to a deeper understanding of how urea application influences plant growth and development, paving the way for optimizing the strategies.

4. Conclusion

This research work demonstrates the potential of urea encapsulated hydrogel beads as a controlled-release system for urea delivery to enhance plant growth and nitrogen uptake in *B. juncea*. Based on our findings, GXG (2%)–U (2%)–SA (1.5) w/v hydrogels represent an effective medium for controlled-release of urea, leading to enhanced plant growth and nitrogen assimilation in *B. juncea*. The experimental design included four treatments: control (C) without urea and hydrogel, direct urea supplementation (U), hydrogel beads with urea (HBWU), and hydrogel beads without urea (HBWOU). The results demonstrated that the hydrogel-mediated delivery of urea significantly increased the biomass, shoot and root length, and total chlorophyll content. While compared with the control plants, the metabolic profiles of HBWU treated plants revealed the upregulation the key metabolites involved in nitrogen metabolism. These findings highlight that the hydrogel system can optimize the availability of nitrogen to the plant, promoting the promising applications of hydrogel-mediated controlled-release systems in agricultural practices for improving plant health and productivity.

Author contributions

B. M.: conceptualization; data curation; formal analysis; methodology; writing – original draft; writing – review and editing; B. V. K.: conceptualization; data curation; formal analysis; methodology; writing – original draft, writing – review and editing; M. K.: formal analysis; methodology; J. K. J. P. K.: formal analysis; methodology; D. S.: formal analysis; methodology; S. F. S.: data curation; formal analysis; funding acquisition; investigation; methodology; project administration; resources; supervision; validation; visualization; writing – review and editing; S. T.H.: resources, M. J. B.: conceptualization; data curation; formal analysis; funding acquisition; investigation; methodology; project administration; resources; supervision; validation; visualization; writing – review and editing. J. Y. C.: data curation; formal analysis; funding acquisition; investigation; methodology; project administration; resources; supervision; validation; visualization; writing – review and editing. All authors have read and agreed to the published version of the manuscript.

Abbreviation

NAD	Nicotinamide adenine dinucleotide
NADP	Nicotinamide adenine dinucleotide phosphate
FTIR	Fourier-transform infrared spectroscopy
GC-MS	Gas chromatography-mass spectrometry
LC-MS	Liquid chromatography-mass spectrometry
KEGG	Kyoto encyclopedia of genes and genomes
HBWU	Hydrogel bead with urea
HBWOU	Hydrogel bead without urea

Data availability

Data for this article, including omics datasets, are available at Figshare at [https://doi.org/10.6084/m9.figshare.27162165]. The data supporting this article have been included as part of the ESI.† E-Supplementary data for this work can be found online alongside the paper.

Conflicts of interest

The authors show no conflict of interest.

References

1 M. Niaounakis, Introduction, In *Biopolymers: Processing and Products, Biopolymers: Processing and Products*, Elsevier, 2015, pp.1–77. , DOI: 10.1016/B978-0-323-26698-7.00001-5.

2 F. G. Torres, O. P. Troncoso, A. Pisani, F. Gatto and G. Bardi, Natural Polysaccharide Nanomaterials: An Overview of Their Immunological Properties, *Int. J. Mol. Sci.*, 2019, **20**(20), 5092, DOI: 10.3390/ijms20205092.

3 H. Zhang, T. Zhao, J. Wang, Y. Xia, Z. Song and L. Ai, An Amendment to the Fine Structure of Galactoxyloglucan from Tamarind (Tamarindus Indica L.) Seed, *Int. J. Biol. Macromol.*, 2020, **149**, 1189–1197, DOI: 10.1016/j.ijbiomac.2020.01.284.

4 X. Guo, Y. Wang, Y. Qin, P. Shen and Q. Peng, Structures, Properties and Application of Alginic Acid: A Review, *Int. J. Biol. Macromol.*, 2020, **162**, 618–628, DOI: 10.1016/j.ijbiomac.2020.06.180.

5　A. Mishra and A. V. Malhotra, Tamarind Xyloglucan: A Polysaccharide with Versatile Application Potential, *J. Mater. Chem.*, 2009, **19**(45), 8528, DOI: **10.1039/b911150f**.

6　M. S. Hasnain, P. Ray and A. K. Nayak, Alginate-Based Interpenetrating Polymer Networks for Sustained Drug Release, *Alginates in Drug Delivery*, Elsevier, 2020, pp. 101–128, DOI: **10.1016/B978-0-12-817640-5.00005-4**.

7　S. Maity, A. Chatterjee and J. Ganguly, Stimuli-Responsive Sugar-Derived Hydrogels: A Modern Approach in Cancer Biology, *Green Approaches in Medicinal Chemistry for Sustainable Drug Design*, Elsevier, 2020, pp. 617–649, DOI: **10.1016/B978-0-12-817592-7.00018-6**.

8　B. Tomadoni, C. Casalongué and V. A. Alvarez, Biopolymer-Based Hydrogels for Agriculture Applications: Swelling Behavior and Slow Release of Agrochemicals, *Polymers for Agri-Food Applications*, Springer International Publishing, Cham, 2019, pp. 99–125, DOI: **10.1007/978-3-030-19416-1_7**.

9　J. Liao, X. Liu, A. Hu, H. Song, X. Chen and Z. Zhang, Effects of Biochar-Based Controlled Release Nitrogen Fertilizer on Nitrogen-Use Efficiency of Oilseed Rape (Brassica Napus L.), *Sci. Rep.*, 2020, **10**(1), 11063, DOI: **10.1038/s41598-020-67528-y**.

10　B. R. Araújo, L. P. C. Romão, M. E. Doumer and A. S. Mangrich, Evaluation of the Interactions between Chitosan and Humics in Media for the Controlled Release of Nitrogen Fertilizer, *J. Environ. Manage.*, 2017, **190**, 122–131, DOI: **10.1016/j.jenvman.2016.12.059**.

11　M. Arkoun, X. Sarda, L. Jannin, P. Laine, P. Etienne, J.-M. Garcia-Mina, J.-C. Yvin and A. Ourry, Hydroponics versus Field Lysimeter Studies of Urea, Ammonium and Nitrate Uptake by Oilseed Rape (*Brassica Napus* L.), *J. Exp. Bot.*, 2012, **63**(14), 5245–5258, DOI: **10.1093/jxb/ers183**.

12　C. O. Dimkpa, J. Fugice, U. Singh and T. D. Lewis, Development of Fertilizers for Enhanced Nitrogen Use Efficiency – Trends and Perspectives, *Sci. Total Environ.*, 2020, **731**, 139113, DOI: **10.1016/j.scitotenv.2020.139113**.

13　H. Yang, J. Menz, I. Häussermann, M. Benz, T. Fujiwara and U. Ludewig, High and Low Affinity Urea Root Uptake: Involvement of NIP5;1, *Plant Cell Physiol.*, 2015, **56**(8), 1588–1597, DOI: **10.1093/pcp/pcv067**.

14　M. Wang, Q. Shen, G. Xu and S. Guo, New Insight into the Strategy for Nitrogen Metabolism in Plant Cells, *International Review of Cell and Molecular Biology*, Elsevier Inc., 2014, vol. 310, pp. 1–37, DOI: **10.1016/B978-0-12-800180-6.00001-3**.

15　D. Bassi, M. Menossi and L. Mattiello, Nitrogen Supply Influences Photosynthesis Establishment along the Sugarcane Leaf, *Sci. Rep.*, 2018, **8**(1), 2327, DOI: **10.1038/s41598-018-20653-1**.

16　N. Limsangouan, N. Milasing, M. Thongngam, P. Khuwijitjaru and W. Jittanit, Physical and Chemical Properties, Antioxidant Capacity, and Total Phenolic Content of Xyloglucan Component in Tamarind (Tamarindus Indica) Seed Extracted Using Subcritical Water, *J Food Process. Preserv.*, 2019, **43**(10), e14146, DOI: **10.1111/jfpp.14146**.

17　N. Limsangouan, C. Charunuch, S. K. Sastry, W. Srichamnong and W. Jittanit, High Pressure Processing of Tamarind (Tamarindus Indica) Seed for Xyloglucan Extraction, *LWT*, 2020, **134**, 110112, DOI: **10.1016/j.lwt.2020.110112**.

18　M. R. Torres, A. P. A. Sousa, E. A. T. Silva Filho, D. F. Melo, J. P. A. Feitosa, R. C. M. de Paula and M. G. S. Lima, Extraction and Physicochemical Characterization of Sargassum Vulgare Alginate from Brazil, *Carbohydr. Res.*, 2007, **342**(14), 2067–2074, DOI: **10.1016/j.carres.2007.05.022**.

19　B. Muthumari, B. V. Kumar, M. Kavitha, J. K. J. P. Kumar, N. Arumugam and M. J. Basu, Optimization of Sodium Alginate-Galactoxyloglucan Blended Hydrogel Beads through Ionotropic Gelation Method, *Int. J. Biol. Macromol.*, 2023, **242**, 124630, DOI: **10.1016/j.ijbiomac.2023.124630**.

20　M. Balakrishnan, V. K. Balasubramanian, K. Murugan, J. P. K. John Kennedy, J. Y. Chou and J. B. Muthuramalingam, Ionically Crosslinked Sodium Alginate – Galactoxyloglucan Hydrogel Beads as a Controlled Release System for Sustainable Urea Delivery, *Mater. Today Commun.*, 2024, **41**, 110912, DOI: **10.1016/j.mtcomm.2024.110912**.

21　E. G. Arafa, M. W. Sabaa, R. R. Mohamed, E. M. Kamel, A. M. Elzanaty, A. M. Mahmoud and O. F. Abdel-Gawad, Eco-Friendly and Biodegradable Sodium Alginate/Quaternized Chitosan Hydrogel for Controlled Release of Urea and Its Antimicrobial Activity, *Carbohydr. Polym.*, 2022, **291**, 119555, DOI: **10.1016/j.carbpol.2022.119555**.

22　M. E. González, M. Cea, J. Medina, A. González, M. C. Diez, P. Cartes, C. Monreal and R. Navia, Evaluation of Biodegradable Polymers as Encapsulating Agents for the Development of a Urea Controlled-Release Fertilizer Using Biochar as Support Material, *Sci. Total Environ*, 2015, **505**, 446–453, DOI: **10.1016/j.scitotenv.2014.10.014**.

23　N. J. Langenfeld, L. E. Payne and B. Bugbee, Colorimetric Determination of Urea Using Diacetyl Monoxime with Strong Acids, *PLoS One*, 2021, **16**(11), e0259760, DOI: **10.1371/journal.pone.0259760**.

24　Y.-R. Chen, C.-Y. Kuo, S.-F. Fu and J.-Y. Chou, Plant Growth-Promoting Properties of the Phosphate-Solubilizing Red Yeast Rhodosporidium Paludigenum, *World J. Microbiol. Biotechnol.*, 2023, **39**(2), 54, DOI: **10.1007/s11274-022-03498-9**.

25　S.-Y. Lee, E.-G. Kim, J.-R. Park, Y.-H. Ryu, W. Moon, G.-H. Park, M. Ubaidillah, S.-N. Ryu and K.-M. Kim, Effect on Chemical and Physical Properties of Soil Each Peat Moss, Elemental Sulfur, and Sulfur-Oxidizing Bacteria, *Plants*, 2021, **10**(9), 1901, DOI: **10.3390/plants10091901**.

26　B. Tomadoni, M. F. Salcedo, A. Y. Mansilla, C. A. Casalongué and V. A. Alvarez, Macroporous Alginate-Based Hydrogels to Control Soil Substrate Moisture: Effect on Lettuce Plants under Drought Stress, *Eur. Polym. J.*, 2020, **137**, 109953, DOI: **10.1016/j.eurpolymj.2020.109953**.

27　M. Pérez-Patricio, J. Camas-Anzueto, A. Sanchez-Alegría, A. Aguilar-González, F. Gutiérrez-Miceli, E. Escobar-Gómez, Y. Voisin, C. Rios-Rojas and R. Grajales-Coutiño, Optical Method for Estimating the Chlorophyll Contents in Plant Leaves, *Sensors*, 2018, **18**(2), 650, DOI: **10.3390/s18020650**.

28　F. Gevi, G. Fanelli, L. Zolla and S. Rinalducci, Untargeted Metabolomics of Plant Leaf Tissues, *Methods in Molecular*

Biology, Humana Press Inc., 2019, vol. 1978, pp. 187–195, DOI: 10.1007/978-1-4939-9236-2_12.

29 S. Liang, D. Gao, H. Liu, C. Wang and J. Wen, Metabolomic and Proteomic Analysis of D-Lactate-Producing Lactobacillus Delbrueckii under Various Fermentation Conditions, *J. Ind. Microbiol. Biotechnol.*, 2018, **45**(8), 681–696, DOI: 10.1007/s10295-018-2048-y.

30 H. Li, M.-L. Ma, S. Luo, R.-M. Zhang, P. Han and W. Hu, Metabolic Responses to Ethanol in Saccharomyces Cerevisiae Using a Gas Chromatography Tandem Mass Spectrometry-Based Metabolomics Approach, *Int. J. Biochem. Cell Biol.*, 2012, **44**(7), 1087–1096, DOI: 10.1016/j.biocel.2012.03.017.

31 M. Xia, D. Huang, S. Li, J. Wen, X. Jia and Y. Chen, Enhanced FK506 Production in Streptomyces Tsukubaensis by Rational Feeding Strategies Based on Comparative Metabolic Profiling Analysis, *Biotechnol. Bioeng.*, 2013, **110**(10), 2717–2730, DOI: 10.1002/bit.24941.

32 Z. Li, M. An, D. Hong, D. Chang, K. Wang and H. Fan, Transcriptomic and Metabolomic Analyses Reveal the Differential Regulatory Mechanisms of Compound Material on the Responses of Brassica Campestris to Saline and Alkaline Stresses, *Front. Plant Sci.*, 2022, 13, DOI: 10.3389/fpls.2022.820540.

33 S. Shen, Y. Tang, C. Zhang, N. Yin, Y. Mao, F. Sun, S. Chen, R. Hu, X. Liu, G. Shang, L. Liu, K. Lu, J. Li and C. Qu, Metabolite Profiling and Transcriptome Analysis Provide Insight into Seed Coat Color in Brassica Juncea, *Int. J. Mol. Sci.*, 2021, **22**(13), 7215, DOI: 10.3390/ijms22137215.

34 B. Vignesh Kumar, B. Muthumari, M. Kavitha, J. K. John Praveen Kumar and M. Jothi Basu, Unraveling the Role of Intra-Cellular Metabolites in the Lactic Acid Production by Novel Bacillus Amyloliquefaciens Using Sugarcane Molasses as a Substratum, *Mol Omics*, 2024, **20**(1), 19–26, DOI: 10.1039/D3MO00141E.

35 T. Ming, J. Han, Y. Li, C. Lu, D. Qiu, Y. Li, J. Zhou and X. Su, A Metabolomics and Proteomics Study of the Lactobacillus Plantarum in the Grass Carp Fermentation, *BMC Microbiol.*, 2018, **18**(1), 216, DOI: 10.1186/s12866-018-1354-x.

36 X. Chen, W. Shu, L. Zhao and J. Wan, Advanced Mass Spectrometric and Spectroscopic Methods Coupled with Machine Learning for in Vitro Diagnosis, *View*, 2023, **4**(1), 20220038, DOI: 10.1002/VIW.20220038.

37 Y. Wang, Y. Liu, S. Yang, J. Yi, X. Xu, K. Zhang, B. Liu and K. Qian, Host–Guest Self-Assembled Interfacial Nanoarrays for Precise Metabolic Profiling, *Small*, 2023, **19**(51), 2207190, DOI: 10.1002/smll.202207190.

38 P. Qu, Y. Li, H. Huang, J. Chen, Z. Yu, J. Huang, H. Wang and B. Gao, Urea Formaldehyde Modified Alginate Beads with Improved Stability and Enhanced Removal of Pb^{2+}, Cd^{2+}, and Cu^{2+}, *J. Hazard. Mater.*, 2020, **396**, 122664, DOI: 10.1016/j.jhazmat.2020.122664.

39 I. R. S. Arruda, P. B. S. Albuquerque, G. R. C. Santos, A. G. Silva, P. A. S. Mourão, M. T. S. Correia, A. A. Vicente and M. G. Carneiro-da-Cunha, Structure and Rheological Properties of a Xyloglucan Extracted from Hymenaea Courbaril Var. Courbaril Seeds, *Int. J. Biol. Macromol.*, 2015, **73**, 31–38, DOI: 10.1016/j.ijbiomac.2014.11.001.

40 P. Tan, C. Zeng, C. Wan, Z. Liu, X. Dong, J. Peng, H. Lin, M. Li, Z. Liu and M. Yan, Metabolic Profiles of Brassica Juncea Roots in Response to Cadmium Stress, *Metabolites*, 2021, **11**(6), 383, DOI: 10.3390/metabo11060383.

41 Y. Zhang, X. Liang, X. Yang, H. Liu and J. Yao, An Eco-Friendly Slow-Release Urea Fertilizer Based on Waste Mulberry Branches for Potential Agriculture and Horticulture Applications, *ACS Sustainable Chem. Eng.*, 2014, **2**(7), 1871–1878, DOI: 10.1021/sc500204z.

42 J. M. Bremner and M. J. Krogmeier, Evidence That the Adverse Effect of Urea Fertilizer on Seed Germination in Soil Is Due to Ammonia Formed through Hydrolysis of Urea by Soil Urease, *Proc. Natl. Acad. Sci. U. S. A.*, 1989, **86**(21), 8185–8188, DOI: 10.1073/pnas.86.21.8185.

43 J. Chen, L. Liu, Z. Wang, Y. Zhang, H. Sun, S. Song, Z. Bai, Z. Lu and C. Li, Nitrogen Fertilization Increases Root Growth and Coordinates the Root–Shoot Relationship in Cotton, *Front. Plant Sci.*, 2020, **11**, 880, DOI: 10.3389/fpls.2020.00880.

44 P. Ebrahimi, Z. Shokramraji, S. Tavakkoli, D. Mihaylova and A. Lante, Chlorophylls as Natural Bioactive Compounds Existing in Food By-Products: A Critical Review, *Plants.*, 2023, **12**(7), 1533, DOI: 10.3390/plants12071533.

45 T. Zhou, Y. Wang, S. Huang and Y. Zhao, Synthesis Composite Hydrogels from Inorganic-Organic Hybrids Based on Leftover Rice for Environment-Friendly Controlled-Release Urea Fertilizers, *Sci. Total Environ.*, 2018, **615**, 422–430, DOI: 10.1016/j.scitotenv.2017.09.084.

46 Z. Chen, Q. Wang, J. Ma, P. Zou and L. Jiang, Impact of Controlled-Release Urea on Rice Yield, Nitrogen Use Efficiency and Soil Fertility in a Single Rice Cropping System, *Sci. Rep.*, 2020, **10**(1), 10432, DOI: 10.1038/s41598-020-67110-6.

47 K. Nishinari, M. Takemasa, K. Yamatoya and M. Shirakawa, Xyloglucan, *Handbook of Hydrocolloids*, Elsevier Inc., 2nd edn, 2009, pp. 535–566, DOI: 10.1533/9781845695873.535.

48 Y. Shen, H. Wang, W. Li, Z. Liu, Y. Liu, H. Wei and J. Li, Synthesis and Characterization of Double-Network Hydrogels Based on Sodium Alginate and Halloysite for Slow Release Fertilizers, *Int. J. Biol. Macromol.*, 2020, **164**, 557–565, DOI: 10.1016/j.ijbiomac.2020.07.154.

49 C.-P. Witte, Urea Metabolism in Plants, *Plant Science*, 2011, **180**(3), 431–438, DOI: 10.1016/j.plantsci.2010.11.010.

50 P. Mérigout, M. Lelandais, F. Bitton, J.-P. Renou, X. Briand, C. Meyer and F. Daniel-Vedele, Physiological and Transcriptomic Aspects of Urea Uptake and Assimilation in Arabidopsis Plants, *Plant Physiol.*, 2008, **147**(3), 1225–1238, DOI: 10.1104/pp.108.119339.

51 H. Zhu, Z. Ye, Z. Xu and L. Wei, Transcriptomic Analysis Reveals the Effect of Urea on Metabolism of Nannochloropsis Oceanica, *Life*, 2024, **14**(7), 797, DOI: 10.3390/life14070797.

52 B. G. Forde and P. J. Lea, Glutamate in Plants: Metabolism, Regulation, and Signalling, *J. Exp. Bot.*, 2007, **58**(9), 2339–2358, DOI: 10.1093/jxb/erm121.

53 V. Cruzat, M. Macedo Rogero, K. Noel Keane, R. Curi and P. Newsholme, Glutamine: Metabolism and Immune

Function, Supplementation and Clinical Translation, *Nutrients*, 2018, **10**(11), 1564, DOI: **10.3390/nu10111564**.

54 X.-M. Qiu, Y.-Y. Sun, X.-Y. Ye and Z.-G. Li, Signaling Role of Glutamate in Plants, *Front. in Plant Sci.*, 2020, **10**, 1743, DOI: **10.3389/fpls.2019.01743**.

55 W. L. Araújo, A. O. Martins, A. R. Fernie and T. Tohge, 2-Oxoglutarate: Linking TCA Cycle Function with Amino Acid, Glucosinolate, Flavonoid, Alkaloid, and Gibberellin Biosynthesis, *Front. Plant Sci.*, 2014, **5**, 552, DOI: **10.3389/fpls.2014.00552**.

56 V. Bandarian, W. J. Poehner and S. D. Grover, Metabolite Activation of Crassulacean Acid Metabolism and C4 Phospho Enol Pyruvate Carboxylase, *Plant Physiol.*, 1992, **100**(3), 1411–1416, DOI: **10.1104/pp.100.3.1411**.

57 J. Shen, W. Wu, K. Wang, J. Wu, B. Liu, C. Li, Z. Gong, X. Hong, H. Fang, X. Zhang and X. Xu, Chloroflexus Aurantiacus Acetyl-CoA Carboxylase Evolves Fused Biotin Carboxylase and Biotin Carboxyl Carrier Protein to Complete Carboxylation Activity, *mBio*, 2024, **15**(5), e03414-23, DOI: **10.1128/mbio.03414-23**.

58 Z.-B. Guan, X.-T. Deng, Z.-H. Zhang, G.-C. Xu, W.-L. Cheng, X.-R. Liao and Y.-J. Cai, Engineering Glucosamine-6-Phosphate Synthase to Achieve Efficient One-Step Biosynthesis of Glucosamine, *ACS Chem. Biol.*, 2024, **19**(6), 1237–1242, DOI: **10.1021/acschembio.4c00144**.

59 Y. Liu, P. Wu, B. Li, W. Wang and B. Zhu, Phosphoribosyltransferases and Their Roles in Plant Development and Abiotic Stress Response, *Int. J. Mol. Sci.*, 2023, **24**(14), 11828, DOI: **10.3390/ijms241411828**.

60 P. J. Unkefer, T. J. Knight and R. A. Martinez, The Intermediate in a Nitrate-Responsive ω-Amidase Pathway in Plants May Signal Ammonium Assimilation Status, *Plant Physiol.*, 2023, **191**(1), 715–728, DOI: **10.1093/plphys/kiac501**.

61 V. Hariharan, T. Denton, S. Paraszcszak, K. McEvoy, T. Jeitner, B. Krasnikov and A. Cooper, The Enzymology of 2-Hydroxyglutarate, 2-Hydroxyglutaramate and 2-Hydroxysuccinamate and Their Relationship to Oncometabolites, *Biology*, 2017, **6**(2), 24, DOI: **10.3390/biology6020024**.

62 H. Straube, J. Straube, J. Rinne, L. Fischer, M. Niehaus, C. Witte and M. Herde, An Inosine Triphosphate Pyrophosphatase Safeguards Plant Nucleic Acids from Aberrant Purine Nucleotides, *New Phytol.*, 2023, **237**(5), 1759–1775, DOI: **10.1111/nph.18656**.